**Title**

Hydrological process controls on nitrogen export during storm events in an agricultural watershed

**Names and present postal addresses of authors**

Rui JIANG, Krishna P. WOLI[1], Kanta KURAMOCHI, Atsushi HAYAKAWA[2], Mariko SHIMIZU, Ryusuke HATANO (Laboratory of Soil Science, Graduate School of Agriculture, Hokkaido University, Sapporo 060-8589, Japan)

**Complete address of corresponding author**

Rui JIANG, Laboratory of Soil Science, Graduate School of Agriculture, Hokkaido University, Kita-Ku Kita-9 Nishi-9, Sapporo, 060-8589, Japan;

Email: jiangrui@chem.agr.hokudai.ac.jp;

Fax: 011-706-2494;

Tel: 011-706-2503

**Division**

Environment

**Contribution**

Full-length paper

**Short running title**

Hydrological process controls N export

Present address: [1]Department of Natural Resources and Environmental Sciences, University of Illinois at Urbana-Champaign, Urbana, IL 61801, USA; and [2]Department of Biological Environment, Akita Prefectural University, Akita 010-0195, Japan

**Abstract**

The dynamic characteristics of nitrogen (N) and suspended solids (SS) were investigated in stream water during four storm events in 2003 at the Shibetsu watershed, eastern Hokkaido, Japan. Analysis showed that total nitrogen (TN), nitrate-N ($NO_3^-$-N), dissolved organic nitrogen (DON), particulate nitrogen (PN), and SS concentrations all peaked sharply during the rising limb of the discharge hydrograph, but peaks of PN and SS were more significant than that of dissolved N. PN and SS consistently displayed clockwise hysteresis with higher concentrations during rising flows, whereas $NO_3^-$-N and DON showed different patterns among storms depending upon the antecedent soil moisture. An M (V) curve, defined as nutrient mass distribution vs. the volume of discharge, showed that a "first flush" of PN, $NO_3^-$-N, DON, and SS was observed, however, the distribution of nutrient loads in the discharge was different. PN and SS had a shorter flushing characteristic time constant ($t_{1/e}$, defined as the time interval required for a decline in nutrient concentrations in discharge water to $e^{-1}$ (37%) of their initial concentrations) but contributed 80% of fluxes during the first 50% of the discharge, while longer flush time ($t_{1/e}$) of $NO_3^-$-N and DON with slowly decreased concentrations led to half loads during the recession of the discharge. These data indicated that the flush mechanisms might be distinguished between particulate nutrients and dissolved N. The analysis showed that concentrations of PN and SS derived from soil erosion were related to surface runoff. In contrast, $NO_3^-$-N originated from the near-surface soil layer associated with the rising shallow ground water table and mainly flushed with

subsurface runoff. Different flushing mechanisms implied that different watershed best management practices should be undertaken for effectively mitigating water quality degradation.

**Key words:** first flush, flow paths, flushing, nitrogen, storm events.

## INTRODUCTION

Quantifying the export of N from catchments has become a significant issue for land managers over the past 20 years. Although many studies have demonstrated that the characteristics of nutrient export are complicated due to a variety of factors, such as geographic, hydrologic, climatic, biochemical, and anthropological factors and although each is not a fundamental process, they drew some conclusions in common. First, N export had a significant variable signal at a temporal scale. In particular, rainfall events and/or snowmelt seasons contributed to high concentrations and fluxes of N (Baron & Campbell 1997; Brooks & Williams 1999; Hatano *et al*. 2005; Inamdar *et al.* 2004; McNamara *et al*. 2008; Mitchell *et al.* 1996; Zhang *et al*. 2007). Second, the flushing of N during a snowmelt season or storm events was observed (Brown *et al*. 1999; Burns 2005; Burns *et al*. 1998; Creed & Band 1998a, 1998b; Creed *et al.* 1996; Inamdar *et al*. 2004; McHale *et al*. 2002; Zhang *et al*. 2007). Last, flow paths had a close relationship with N export (Jia *et al*. 2007; Jiang *et al*. 2008; Zhang *et al*. 2007).

There has been considerable interest in identifying the sources, flow paths, and transport mechanisms responsible for the export of N, especially $NO_3^-$-N, within watersheds at the seasonal and rainfall event scale. These studies have resulted in an improved understanding on some of the processes but many are not yet clearly understood. The mechanisms of $NO_3^-$-N export are usually explained by contradictory processes. Creed and Band (1998a, b) found a clockwise, discrete hysteresis pattern of $NO_3^-$-N concentration from glaciated catchments in the Canadian Shield, and attributed

this pattern to the flushing of $NO_3^-$-N from near-surface soil layers due to the rising of groundwater table, but they didn't find any proof of the source of $NO_3^-$-N. In contrast, Brown *et al*. (1999), Inamdar et *al*. (2004), and McHale *et al*. (2002) believed that $NO_3^-$-N export occurred via deep flow paths and the rise in $NO_3^-$-N concentrations were associated with the rapid displacement of till water by infiltrating precipitation. Hill et *al*. (1999) indicated that the biogeochemistry of the organic horizon could regulate the patterns of $NO_3^-$-N loss in subsurface runoff movement by preferential flow pathways in forest soils. Ocampo *et al*. (2006) explained that the dynamic of the shallow ephemeral perched aquifer drove a shift from hydrological controls on $NO_3^-$-N discharge during the "early flushing" stage to an apparent biogeochemical control on $NO_3^-$-N discharge during the "steady decline" stage of the flushing response.

Less attention has been paid to dissolved organic N (DON) compared with $NO_3^-$-N. Recent studies suggest that contributions of DON can be significant and constitute a major portion of the total N solute export (Campbell *et al*. 2000; Willett *et al*. 2004). Although stream nitrate and DON may originate from similar shallow subsurface and surface flow paths during storm events, differences in flushing response among $NO_3^-$-N and DON were found (Cooper *et al*. 2007; Sebestyen *et al*. 2008).

In spite of numerous investigations on N dynamics, studies on the relationship between distribution of N fluxes and stream discharge in agricultural or forested watersheds during storm events are scarce. Quantification of nutrient fluxes in sewage systems and urban watersheds indicated that those watersheds presented strong "first

flush" for most storms and constituents (Barco *et al*. 2008; Bertrand-Krajewski *et al*. 1998; Lee *et al*. 2002). In general, the term "first flush" has been used to indicate that the mass emission rate is higher during the initial portions of runoff than during the last portion (Kondolf & Wilcock 1996; Lee *et al*. 2002). This characteristic of "first flush" has been mentioned to define different pathways for particulate nutrients and dissolved nutrients (Jiang *et al*. 2009) or to use for watershed best management practices (BMPs), such as enhancement of sediment and nutrient removal efficiency by treating the first stage of runoff using sedimentation devices or filters (i.e. ditches, tanks, and ponds) (Barco *et al*. 2008).

Several studies looked at the N export in Shibetsu watershed (Hayakawa *et al.* 2006; Hayakawa *et al.* 2009; Nakata *et al.* 2008, unpublished data; Woli *et al.* 2004). Hayakawa *et al.* (2009) reported that the net N input (NNI) amounted to 55 kg N $ha^{-1}$ $yr^{-1}$ in the Shibetsu watershed and the N export from the watershed outlet accounted for 27% of the NNI. Some studies indicated that land use had a significant positive correlation with $NO_3^-$-N export and agricultural N was a dominant source (Hayakawa *et al.* 2006; Woli *et al.* 2004). However, these studies do not focus on the mechanisms controlling N export to streams at a high temporal resolution during storm events. Therefore, this study highlights on the dynamic concentrations and flux distribution of N in discharge during storms. The objectives of this study are to 1) assess the temporal patterns of N concentrations during storm events, 2) evaluate the distribution of N fluxes in discharge within a storm, 3) clarify whether the flushing of N-export exists

among $NO_3^-$-N, DON, and PN and what is the variation, and (4) examine the potential sources of N export from the Shibetsu watershed.

## MATERIALS AND METHODS

### Watershed description

The Shibetsu watershed is located in eastern Hokkaido (outlet as shown in Fig. 1; 43.634N, 145.085E), Japan. The watershed area is 679 $km^2$, and the upper parts dominated by forest are covered by Volcanogenous Regosols, while the downstream areas are mainly used for agricultural purposes and are covered by Cumulic Andosols, Gray Lowland Soils, and Peat Soils. The topographical characteristic of the region has a mean slope of 4.28° with a maximum value of 34°. The slopes are more gentle and concave in downstream areas than that in upstream. This region has a hemi-boreal climate, characterized by warm summers and cold winters. Precipitation averages 1147 mm $yr^{-1}$ and the annual mean temperature is 5°C, with the lowest mean monthly temperature in February (-8.3°C) and the highest mean monthly temperature in August (18.0°C) (1978-2002 average, Japan Meteorological Agency 2007, http://www.jma.go.jp). The watershed consists of agriculture (51.4%), forest (45.6%), urban area (1.4%), and waste land and road (1.6%). The Nakashibetsu town, covering most of the Shibetsu watershed, has a large grassland area, and dairy farming is a main occupation. The dominant vegetation in forest is Japanese larch-*Larix kaempferi*. Grassland (covered by *Phleum pratense*) occupies more than 95% of the agricultural land area, and the remaining is cultivated with maize (*Zea mays* L.), sugar beet

(*Saccharum officinarum*), potato (*Solanum tuberosum*), and Japanese radishes (*Raphanus sativus Linn.*). The human population was estimated at 24000 persons (35 people $km^{-2}$) concentrated in the middle part of the watershed.

**Watershed monitoring, sampling, and analysis**

Base flow water samples were grabbed from the stream outlet in 1 L polypropylene bottles once a month from March to November in 2003. An automated water sampler (ISCO ™ 3700) was installed at the outlet of Shibetsu watershed, and water samples were collected during four storm events: June 20 (E1), July 11 (E2), September 30 (E3), and October 23 (E4) in 2003. The auto-sampler was triggered when the rainfall was > 4 mm 30 $min^{-1}$ with intervals of 15 min to 1 h during the rising stage of discharge, while 2 to 6 h during the receding section. Water samples were transported to the laboratory quickly after a storm and then stored at 4°C before analyses. Rainfall was measured by a tipping-bucket rain gauge (0.2 mm) placed in an open area near the automated sampler. Daily stream water stage measured every 10 min was obtained from the website of Ministry of Land, Infrastructure and Transport, Japan (http://www1.river.go.jp). Discharge was calculated using calibrated formulas based on the monitoring by local government. Groundwater wells in near-stream forests were constructed of 5 cm (ID) PVC pipes and groundwater levels were recorded using pressure transducer and capacitance water level probes at 10 min intervals. A shallow groundwater well was cored to the depth of 2.94 m under the ground surface where a coarse sandy sediment layer was intersected. A deep groundwater well with a depth of 12.52 m was cored to

the aquifer of Mashu pumice layer. Soil samples were collected once in August 2008 at 27 sites representing most of the watershed area. Each sample was taken in triplicate with an auger from depths of 0-20, 20-50, and 50-100 cm. The triplicate samples from each depth were homogenized before analysis.

Suspended solids (SS) were measured from 800 ml subsamples that were filtered through pre-weighed glass microfiber filters (47 mm, Whatman GF/F). The filters were dried at 90°C for 24 h and weighed again. Total N (TN) was determined by the method of alkaline persulfate digestion and HCl acidified UV detection. After filtering through 0.2 μm membrane filters, water samples were used for analyzing total dissolved N (TDN), $NO_3^-$-N, $NO_2^-$-N, $NH_4^+$-N, and Si. Concentrations of TN and TDN were determined by the method of alkaline persulfate digestion and HCl-acidified UV detection. $NO_3^-$-N and $NO_2^-$-N were determined by ion chromatography (QIC Analyzer; Dionex, Sunnyvale, CA); $NH_4^+$-N was determined by colorimetry using the indophenol blue method; and Si was determined colorimetrically by the molybdenum blue method. Particulate N (PN) and DON were calculated by subtracting the concentration of TDN from TN, and inorganic N ($NO_3^-$-N, $NO_2^-$-N, $NH_4^+$-N) from TDN, respectively. Soil samples were air dried and ground to pass a 2 mm sieve for $NO_3^-$-N analysis. $NO_3^-$-N in soil was extracted using a 1:5 soil:2 M KCl solution and the concentrations were determined by colorimetry.

**Data analysis**

For examining the variation in water chemistry, we performed Kruskal-Wallis test and

multiple comparisons by Steel-Dwass test.

*Antecedent precipitation index*

Several researchers have used relative antecedent precipitation index (API) values to compare soil moisture among pre-storm conditions (Christopher *et al*. 2008; Inamdar & Mitchell 2006; McDonnell *et al*. 1991). The API index was calculated for the four storm events in our study, which is defined as:

$$API_x = \sum_{i=1}^{x} \frac{p_i}{i}$$

where $x$ = 7 and 21 days before a rain event and $P_i$ (mm) is the total precipitation on the $i^{th}$ day before the event. We used $API_7$ for calculating the surface soil moisture and $API_{21}$ for the deep groundwater situation, because the surface Volcanogenous soil usually has high infiltration rates and can quickly get into the shallow groundwater aquifer. But when the water seeps into deeper soil layer through the coarse sandy sediment layer, it needs longer time.

*Runoff coefficient*

The runoff coefficient is defined as the total volume of discharge divided by the total volume of precipitation (amount of precipitation multiplied by watershed area), which is another indicator of wetness in the watershed.

*Time constant*

A time series of discharge and the concentration of N in discharge highlight the export behavior of N from a watershed. We presumed an exponential decline in N concentrations during the receding limb of the discharge. According to Creed and Band

(1998a), this decline can be described by:

$$N_t = N_0 e^{-kt}$$

where $N_t$ is the concentration of N in the discharge waters at time=$t$, (mg $L^{-1}$). $N_0$ is the concentration of N in the discharge waters at $t$=0, the time that peak concentration of N is observed (mg $L^{-1}$). $t$ is time in h and $k$ is the constant proportionality factor ($h^{-1}$). A time constant ($t_{1/e}$) is defined as the time interval that must elapse in order for the concentrations of N in the discharge waters to decline to $e^{-1}$ (37%) of their initial concentration.

*M (V) curve and mass first flush ratio*

The M (V) curve, which is described as the normalized load ($M_i$) vs. normalized water discharge volume ($V_i$), was used to analyze the load distribution in discharge (Bertrand-Krajewski *et al.* 1998).

$$M_i = \frac{\sum_{i=1}^{j} C_i Q_i \Delta t_i}{\sum_{i=1}^{N} C_i Q_i \Delta t_i}, \quad V_i = \frac{\sum_{i=1}^{j} Q_i \Delta t_i}{\sum_{i=1}^{N} Q_i \Delta t_i}$$

where $N$ is the total number of measurements, $j$ is the index from 1 to $N$. $C_i$ and $Q_i$ are instantaneous concentration and water discharge. If the M (V) curve is above the bisector, "first flush" phenomenon occurs (Geiger 1987; Saget *et al.* 1995) and the magnitude of the first flush can be quantified for each storm and for each water quality parameter using a mass first flush (MFF) ratio (Barco *et al,* 2008). The MFF ratio was calculated as:

$$MFF_n = \frac{M_i}{V_i}$$

where n is the index in the storm corresponding to the percentage of the water discharge, ranging from 0% to 100%. By definition, MFF ratio equals zero in the beginning of a storm and it always equals 1.0 at the end of the storm. The MFF ratio is a useful tool for quantifying first flush and can be statistically characterized or used in regressions or other investigations to understand the magnitude of a first flush and storm or catchment characteristics. For example, an $MFF_{20}$ equal to 2.5 means that 50% of the mass is contained in the first 20% of the discharge water.

Additionally, measurements of the $NO_3^-$-N and $NH_4^+$-N concentrations in bulk rainfall samples during different storm events showed very low concentrations (i.e. $NO_3^-$-N was below 0.15 mg $L^{-1}$; $NH_4^+$-N was below 0.2 mg $L^{-1}$). Therefore, the atmospheric input of N with rainfall was not considered as an important source of stream water N during the hydrological events.

## RESULTS

### Hydrological storm events

The hydrological characteristics of the four storm events varied considerably (Table 1). The total amount of rainfall ranged from 50 mm to 91 mm. Although a single peak was observed for all events (Fig. 2), the peak discharges varied from 51.4 $m^3 s^{-1}$ to 167.7 $m^3 s^{-1}$(Table 1). Fast hydrological response of the watershed to rainfall was reflected in the length of time to the peak ($T_p$, time from the start of rain to the peak of stream water discharge). The longest $T_p$ was found in E2, which had the lowest antecedent

precipitation index ($API_7$) value (Table 1). In contrast, E3 with the highest antecedent soil moisture (19.3 for $API_7$ and 28.4 for $API_{21}$) had the shortest $T_p$ (Table 1). The runoff coefficient increased with an increase in the value of $API_{21}$, except for E4; but it also increased with the increase in groundwater level, except for E3, during four storms from early summer to autumn (Table 1, Fig. 2), suggesting the antecedent soil moisture together with the seasonal factors could have controlled the watershed wetness.

The groundwater level in near-stream forests was analyzed since it might be critical to describe evolution of solute signatures during the storm events. The focus here was on the temporal response of groundwater level in near-stream forests vs. stream discharge. The shallow and deep groundwater level along with discharge and precipitation are presented in Fig. 2. Groundwater level during storm events indicated surface saturation and deep seepage in the near-stream forests. Importantly, these water levels showed that: (a) the maximum of shallow groundwater level just occurred at the precipitation peak and before the stream discharge peak, implying the shallow groundwater quickly responded to the rainfall and contributed to the stream discharge; (b) deep groundwater was raising slowly at the rising limb of discharge, but kept increasing after the recession of discharge; and (c) surface saturation was maintained even after precipitation cessation and during the recession of discharge.

**Comparison in N concentrations between storm events and base flow**

Nutrients and SS concentrations in base flow were different among constituents (Table 2), The most prevalent form of N was $NO_3^-$-N (54% of TN, 59% of DTN, and 95% of

DIN). DON accounted for 36% of TN, and PN only 9% of TN. The concentrations during storm events were highly variable among N species. The dominant form during the storm events was not only $NO_3^-$-N but also PN. $NO_3^-$-N accounted for 8-70% of TN with an average of 37%, 27%, 50%, and 45% for E1, E2, E3, and E4, respectively; while PN accounted for 0-86% of TN depending primarily on the peak discharge, with the average of 46%, 57%, 20%, and 21% for each storm event. The PN : $NO_3^-$-N ratio ( Fig. 3) showed that PN was the dominant form on the rising limb of the discharge, and an increase in rainfall amount increased the length of the dominant time (i.e. E2); while $NO_3^-$-N was dominant on the receding limb. DON ranked second ranging from 15 to 34% during the storm period. $NH_4^+$-N concentrations were very low as base flow, and were below the detection limit in many samples. According to Kruskal-Wallis H and Steel-Dwass test (Table 2), discharge, SS, PN, and $NH_4^+$-N all showed significant difference among storm events and base flow. However, $NO_3^-$-N and DON only showed difference among storm events; while TN didn't show any difference. In brief, the concentrations of all forms of N (except for $NH_4^+$-N and $NO_2^-$-N) were significantly higher than those observed in forested watersheds, regardless of the base flow or storm events.

**Dynamic concentrations of N during storm events**

The concentrations of TN, PN, and SS changed notably and had similar patterns in all storm events, which peaked sharply during the rising limb of discharge and then dropped rapidly (Fig. 4). TN and PN concentrations are shown in Table 2 and Fig. 4. A

significant positive correlation was found between TN and PN ($R^2$=0.98, p<0.001). PN and SS also had a significant positive correlation ($R^2$=0.89, p<0.001). The dissolved N concentrations didn't show significant changes, although the peak concentrations also occurred before the discharge peaked. $NO_3^-$-N concentrations varied slightly with ranges of 0.5-0.8, 0.3-0.7, 0.5-1.0, and 0.4-0.8 mg $L^{-1}$, while DON concentrations ranged 0.1-0.6, 0.1-0.5, 0.2-0.8, and 0.3-0.7 mg $L^{-1}$ during the storms. The maximum value of PN in E2 was much larger than those in other storm events, which could probably be due to antecedent dry soil condition (low $API_7$ value, Table 1).

The peaks of dissolved N followed the peaks of shallow groundwater level or after the water table elevated to a certain level (Fig. 4). This corresponding response was most obvious in E3, when concentrations of $NO_3^-$-N and DON both showed two peaks corresponding to the shallow groundwater level hydrograph; while PN did not show the second peak similar to dissolved N. Therefore we speculated that dissolve N was sensitive to the change in shallow groundwater.

**Discharge-concentration patterns and responses of N export during rising and receding lamb of hydrograph**

Although N and SS all peaked before the discharge peaks, the relationships between concentrations and discharge were different. PN and SS displayed consistently clockwise hysteresis in all storm events, whereas dissolved N showed no consistent pattern among storms. Counter-clockwise concentration-discharge relationships of $NO_3^-$-N and DON were found in E1, no hysteresis in E3, and clockwise hysteresis

existed in E2 and E4 (Fig. 5).

Discharge-weighted mean concentrations of nutrients and rainfall conditions during each rising section of period have been analyzed to investigate the runoff mechanisms. Table 3 shows that nutrient concentrations had significant positive correlation with the cumulative rainfall, whereas no uniform correlation with rainfall intensity in the storm events.

As we observed that N and SS concentrations all peaked quickly during the rising section of discharge and declined during the receding section, we investigated the dynamic characteristics of concentrations during the receding limb of the discharge hydrograph to determine the flow path contributions in a catchment and potential N export affected by a storm event. The $t_{1/e}$ values of PN and SS were shorter than dissolved N, and $t_{1/e}$ for $NO_3^-$-N was the longest (Table 4). The reason could be that PN and SS were likely flushed away by overland flow and dissolved nutrients could have been removed by both surface and subsurface flow (Zhang *et al*. 2007). Moreover, we noticed that the $t_{1/e}$ for all nutrients were longer in E1 than other storms and the longer time of export might have led to more loads of nitrate.

**The M (V) curves of N loads distribution vs. discharge during storm events**

The M (V) curve helps to understand the nutrient mass distribution vs. the water discharge volume relationship. Figure 6 shows the normalized loads of N and SS as a function of normalized discharge for the four storm events. All curves were above the bisector, which showed the “first flush” of constituents. The PN and SS curves were

above the curves of $NO_3^-$-N and DON, indicating a stronger first flush for particulates, probably because PN and SS associated with soil erosion were more prone to move during the early stage of storm.

In order to quantify the magnitude of first flush and analyze load distribution, the first flush ratios ($MFF_{30}$ and $MFF_{50}$) were used. Table 5 shows that the $MFF_n$ of PN and SS were higher than that of $NO_3^-$-N and DON. On average, $NO_3^-$-N, DON, TN, PN and SS transported 35%, 39%, 49%, 66%, and 71% of the total loads in the first 30% of the water discharge during the four storms, respectively; and 56%, 63%, 70%, 80%, and 88% of loads for the first 50% of the water discharge. These data indicated that the first flush of dissolved N was weaker than PN and SS and the contributions of first flush to the export loads were different between particulate nutrients and dissolved N, which might be ascribed to different flush mechanisms for the different forms of N in a watershed.

**Contribution of storm events to annual N loads**

We estimated the loads of N and SS during the storm events and found that TN accounted for 27.7% and $NO_3^-$-N, DON, PN, and SS accounted for 16.2%, 24.7%, 45.4%, and 37.2%, respectively of the total annual loads during the four storms (Table 6). The largest storm, E2 with the lowest value of $API_7$, contributed the largest loads, especially PN and SS.

## DISCUSSION

### Impact of hydrologic characteristics

Antecedent soil moisture is one of the most important factors for watershed hydrological response to rainfall. A previous study (Rusjan *et al.* 2008) showed that higher API value could cause a faster hydrological response (shorter $T_p$). Comparing the $API_7$ and $API_{21}$ values of our study, the value of $API_7$ was more consistent with the previous study, suggesting that the hydrological response depended more on the antecedent soil moisture of shallow groundwater aquifer than the deep groundwater level. But our study showed that the $T_p$ was longer than other headwater streams probably due to the bigger size of our watershed (Rusjan *et al*. 2008; Zhang *et al.* 2007, 2008). The shallow groundwater level showed that the saturation in near-stream areas was dictated by antecedent moisture condition (i.e. ponding in E3 with highest API value and antecedent groundwater level, Fig. 2; Table 1) and the shallow groundwater might be recharged by subsurface flow and return flow from contributing hill slopes and those flows were most likely responsible for the continued saturation of the near-stream areas even after precipitation cessation and hydrograph recession (i.e. E1 and E2, Fig. 2). Thus, subsurface flow could dominate the receding limb of the hydrograph and might be a big contributor to $NO_3^-$-N export.

Runoff coefficient is another indicator of wetness in a watershed, which reflects not only antecedent soil moisture, but also other factors such as evapotranspiration, growth of vegetation, plant cover, etc. Our increasing values of runoff coefficient from summer to autumn seemed to imply that the plant growth and evapotranspiration processes also played an important role in watershed hydrological cycle, except for the increasing

groundwater level. The highest API and antecedent groundwater level both were observed in E3, but the largest runoff coefficient was in E4. This might be related to the decrease in water use by plants and evaporation in autumn.

Rainfall intensity was found to have negative correlation with $NO_3^-$- N, but a positive correlation with PN (Zhang *et al*. 2008). However, there was no correlation between nutrients and rainfall intensity in our study, probably owing to the lag of hydrological response to rainfall (longer $T_p$, Table 1). The correlation between nutrient concentrations and cumulative rainfall showed that the amount of rainfall was a controlling factor for nutrient export in the Shibetsu watershed. To analyze the correlation between nutrient concentrations and rainfall intensity, further monitoring needs to be conducted in the headwater stream.

**Major sources of PN, $NO_3^-$-N, and DON**

Temporal changes in stream chemistry reflect the sequence in which hydrological flow paths link source areas to streams. As catchment wetness increases during storm events, the nutrients in the stream reflect the sources that are available and the amount of water that flows through the source areas of those nutrients. Although concentrations of $NO_3^-$-N, DON, and PN all were larger on the rising limb of the discharge hydrograph, the differences including the export time, the export patterns, and the export load distribution in the discharge imply that they could have resulted from different sources with different export mechanisms.

Previous studies have reported a significant positive correlation between nutrient

concentrations and discharge, and these relationships varied depending on study sites as well as rain events (Ahearn *et al*. 2004; McNamara *et al*. 2008). Our study showed that different patterns not only existed among storm events but also different nutrients at the same study site, which implied a variation in a mechanism of nutrient export. PN always with clockwise patterns and significant "first flush" indicated that it was mainly sourced from the surface flow due to soil erosion, and a significant correlation with SS could have been evidence. In contrast, the patterns of dissolved N were variable associated with different shallow groundwater level or antecedent soil moisture, and the "first flush" was very weak. Thus transport of dissolved N might be better related to subsurface runoff or groundwater which is always affected by shallow aquifer or antecedent soil moisture. Therefore, we speculated that PN could have been derived from the surface soil while dissolved N appeared to be mainly transported by subsurface flow or originated from groundwater.

Inamdar *et al*. (2004) believed that $NO_3^-$-N export occurred via deep flow paths and the rise in $NO_3^-$-N concentrations were associated with the rapid displacement of till water by infiltrating precipitation, using base cations ($Ca^{2+}$ and $Mg^{2+}$) as indicators. McHale *et al*. (2002) and Iqbal (2002) also reached a similar conclusion. We used Si as an indicator, which is regarded as only deriving from rock weathering in a deep layer, and the result is shown in Fig. 7. An opposite trend was found between Si and $NO_3^-$-N concentrations, which was different from the parallel trends (Inamdar *et al*. 2004), implying that $NO_3^-$-N was not from deep groundwater; and the mechanism must differ

from the explanation of Inamdar *et al*. (2004).

Creed and Band (1998a) attributed the early peaks in the $NO_3^-$-N concentration to the "flushing" hypothesis, in which nutrients are leached from near-surface layers by a rising water table followed by a quick lateral transport of these leached nutrients to the stream via near-surface subsurface stormflow on the hillslope and/or surface, saturation excess runoff in the riparian zone. Hydrologically, a key feature of this perceptual model is full-column saturation of the soil profile or water table rises high enough into the soil profile to encounter near-surface soils with high transmissivity and thus the potential for significant lateral flow to occur. This 'transmissivity feedback' has now become a common hypothesis to explain lateral flushing of labile nutrients (Bishop *et al.* 2004). In our study, we observed the shallow groundwater level to raise above 20 cm depth under the soil surface during the storm events, and above ground surface at the wet antecedent condition in E3 (Fig. 2). This indicates that the requirement of hydrology for $NO_3^-$-N flushing was met in our study. In addition, a key requirement of the "flushing" hypothesis biogeochemically also exists, that is the ready availability of excess nutrients in the near surface soil horizons (Qualls & Haines 1991; Weiler & McDonnell 2006). Previous studies found a highly significant positive correlation between $NO_3^-$-N concentrations in stream water and the proportion of upland area in Shibetsu watershed under a baseflow condition (r=0.89, Hayakawa *et al*. 2006; r=0.84, Woli *et al*. 2004), which indicated that the area of uplands was the most important factor for determining $NO_3^-$-N concentrations. Woli *et al*. (2004) also stated that the

regression coefficient had a significant positive correlation with the cropland surplus N, chemical fertilizer N, and manure fertilizer N. Meanwhile, our soil chemical analysis revealed that $NO_3^-$-N concentration in 0-20 cm depth of soil layer was significantly higher than that of 20-50 cm and 50-100 cm depths (Fig. 8). These studies above all indicated that the higher N application rates resulted in the greater field surplus N accumulated in the top 0-20 cm soil layer and had the potential to leach into the stream in the Shibetsu watershed. In addition, local famers usually apply fertilizer on grasslands in spring and summer, and apply manure in spring or autumn (the annual application rate of chemical fertilizer N is 80 kg $ha^{-1}$ and an equal amount of manure fertilizer N is added, Agricultural Department of Hokkaido Government, 2002), which had a high risk of $NO_3^-$-N leaching during the rainy seasons if fertilizer management was not appropriate (Jia *et al*. 2007). Thus, we believe that the source area of $NO_3^-$-N flushing was variable in the near-surface soil layer in upland areas due to the rising shallow groundwater level. Shallow groundwater level consistently reached a maximum (closest to the soil surface) before peak of $NO_3^-$-N concentration and discharge (Fig. 4) thus supporting the flushing of $NO_3^-$-N.

On the basis of the variable source area (VSA) concept, for a given watershed, N flushing may have been regulated not by the total VSA but by the rate of change in the expanding source area (*dVSA/dt*). Although the rate that would have been regulated by topography (Creed & Band 1998a), we believe that the rate also may be regulated by antecedent shallow groundwater level which affects the water connectivity of the

**Deleted:** source area ($A_{VSA}$)

**Deleted:** $dA_{VSA}$

watershed in a rain event and may lead to a different *dVSA/dt*. For example, E1 needs longer time to connect the hydraulic connectivity well because of the shallow groundwater level and dry antecedent soil moisture, which makes $NO_3^-$-N flux moving slower from the variable source areas at the first stage (smaller values of *dVSA/dt*). This may be one of the reasons to explain the counterclockwise direction of the hysteresis loops of E1 as a "prolonged flushing mechanism" (Weiler & McDonnell 2006; Rusjan *et al.* 2008).

Deleted: $dA_{VSA}$

Deleted: $dA_{VSA}$

A similar pattern of concentrations between DON and $NO_3^-$-N in all storm events was observed in our study (Fig. 9). Several studies found the DON peaks on the rising limb similar to our finding (Buffam *et al*. 2001; Hill 1999; Inamdar & Mitchell 2007; McHale *et al*. 2000; Vanderbilt *et al*. 2003). However, Vanderbilt *et al*. (2003) attributed this pattern to the flushing of decomposing leaf litter; Inamdar and Mitchell (2007) and Hill (1999) reported that the stream DON were derived from throughfall. In contrast, Hagedorn *et al*. (2000, 2001) found DON peaks on the recession limb and attributed this to mobilization of DON during its passage through the forest canopy and organic-rich topsoil. In the case of Shibestu watershed, we just found the DON peaked after a maximum value of shallow groundwater level and the trends of DON and shallow ground water level were very similar, especially in E3 (Fig. 9). Therefore, we speculate that it may correlate with ground water rising, and that it may lead to flushing just like $NO_3^-$-N. However, we have no evidence to confirm the source of DON, owing to the lack of analyses of throughfall, litter, and soil water. However, we noticed that the

concentrations of DON in E3 and E4 (in autumn) were significantly higher than that in E1 and E2 (Table 2). Hagedorn *et al*. (2001) attributed the high DON exports to elevated decomposer activity and availability of fresh leaf litter in fall. While Hayakawa *et al*. (2006) reported a positive relationship between upland area (grassland area) and DON concentrations in the Shibetsu watershed. Decomposing of grass litter and manure application in autumn could be the reason for the relationship. Thus our finding may confirm the flushing of decomposed leaf litter on the forest and decomposed manure and leaf litter on the grassland.

**Implication of the "first flush" for watershed management**

Two observations about the "first flush effect" in our study may have important implication for the management of water resources: (1) high concentrations and fluxes of SS and PN exported rapidly for a short time at the beginning of discharge; and (2) slow recession of nitrate concentration and long flushing time in the falling limb lead to half of the $NO_3^-$-N flux export. The higher initial SS and PN concentrations early in the runoff that are associated with a first flush have important interaction with the removal efficiency of the best management practice (BMP). It has been noted that many BMPs, such as ponds and wetlands, operate at great efficiency in removing particles including PN during storm events if the pond or wetlands can effectively reduce the nutrients that are transported at the rising limb of discharge during the first flush (Luo 2008). Gentle sloping landform has the potential to last long time of water retention; and agricultural landscapes have typically been found to leach greater amounts of $NO_3^-$-N (Hayakawa *et*

*al*. 2006; Woli *et al*. 2004). Geologic characteristics associated with agricultural operations in Shibetsu watershed might lead to a long flushing time of $NO_3^-$-N, which would likely contribute to a much higher $NO_3^-$-N concentration and flux to the water body. Thus appropriate fertilizer management in summer and autumn in the Shibetsu watershed, where the rainfall is rich during these seasons, is apparently crucial for preventing excess N losses to stream during storm events. In addition, Hayakawa *et al*. (2006) studied the impact of wetland on $NO_3^-$-N concentration by comparing Shibetsu watershed with another wetland watershed and found that wetland played an important role in attenuation of $NO_3^-$-N. The spatial distribution of wetland or riparian areas in the watershed and their connectedness with the stream network will be a key for delivery of $NO_3^-$-N and thus regulate the flushing response. However, this application must be carefully undertaken because the regulation of wetlands or riparian forests on $NO_3^-$-N flushing is complicated (Inamdar & Mitchell 2006).

**Conclusions**

Although concentrations of N and SS all peaked at the rising limb of discharge, PN and SS consistently displayed clockwise hysteresis between concentration and discharge and showed a short flush time constant ($t_{1/e}$), while dissolved N showed long $t_{1/e}$ and different patterns among storms associated with antecedent soil moisture. These differences indicated that particulate N originated from the surface soil and was transported by surface flow. In contrast, dissolved N was related to subsurface flow. $NO_3^-$-N was leached from near-surface soil layers by rising water table followed by a

quick lateral transport of the leached $NO_3^-$-N to the stream via subsurface flow on the cropland. Although concentration patterns of DON and $NO_3^-$-N were similar, DON could have been closely related to the ground water rising and decomposed leaf litter and manure. Further study is required to take throughfall, litter, and soil water into consideration.

Although the first flush of N and SS were observed, PN and SS were more significant and contributed 80% of fluxes at the first 50% of the discharge, whereas dissolved N with slowly decreased concentrations led half loads to export during the recession of the discharge. The different flushing mechanisms between particulate nutrients and dissolved N implied that different BMPs should be conducted for effective mitigation of N export on a watershed scale.

**ACKNOWLEDGMENTS**

We thank Dr. Toshiya Saigusa, Mr. Osamu Sakai, Mr. Hiroyuki Koda, and Mr. Toshinobu Koba, Hokkaido Konsen Agricultural Experiment Station, for their help and suggestions on this study. This study was partly supported by a Japanese Grant-in-Aid for Science Research from the Ministry of Education, Culture, Sports, Science and Technology (No.14209002 and No.19201008) and The Strategic International Cooperative Program "Comparative Study of Nitrogen Cycling and Its Impact on Water Quality in Agricultural Watersheds in Japan and China" by the Japan Science and Technology Agency. The research grant was provided by the "Hokkaido Regional Development Bureau for the Restoration Project in the Shibetsu River" and Global COE program "Establishment of Center for Integrated Field Environmental Science", MEXT, Japan.

**Deleted:** the "Global COE research grant for young scientists"

**REFERENCES**

Ahearn DS, Sheibley RW, Dahlgren RA, Keller KE 2004: Temporal dynamics of stream water chemistry in the last free-flowing river draining the western Sierra Nevada, California. *J. hydrol.* **295,** 47-63.

Agricultural Department of Hokkaido Government. Standard fertilizer application for Hokkaido 2002; Sapporo (in Japanese).

Barco J, Papiri S, Stenstrom MK 2008: First flush in a combined sewer system. *Chemosphere* **71,** 827–833.

Baron JS, Campbell DH 1997: Nitrogen fluxes in high elevation Colorado Rocky Mountain Basin. *Hydrol. Process.* **11,** 783–799.

Bertrand-Krajewski J-L, Chebbo G, Saget A 1998: Distribution of pollutant mass vs volume in storm water discharges and the first flush phenomenon. *Water Res.* **32 (8),** 2341–2356.

Bishop K, Seibert J, Kohler S, Laudon H 2004: Resolving the double paradox of rapidly mobilized old water with highly variable responses in runoff chemistry. *Hydrol. Process.* **18 (1)**, 185–189.

Brooks PD, Williams MW 1999: Snowpack controls on nitrogen cycling and export seasonally snow-covered catchments. *Hydrol. Process.* **13,** 2177–2190.

Brown VA, Mcdonnell JJ, Burns DA, Kendall C 1999: The role of event water, a rapid shallow flow component, and catchment size in summer stormflow. *J. Hydrol.* **217,** 171–190.

Buffam I, Galloway JN, Blum LK, McGlathery KJ 2001: A stormflow/baseflow comparison of dissolved organic matter concentrations and bioavailability in an Appalachian stream, *Biogeochemistry* **53,** 269–306.

Burns DA, Hooper RP, McDonell JJ, Freer JE, Kendal C, Beven K 1998: Base cation concentrations in subsurface flow from a forestedhillslope: the role of flushing frequency. *Water Resour. Res.* **34,** 3535–3544.

Burns DA 2005: What do hydrologists mean when they use the term flushing? *Hydrol. Process.* **19,** 1325–1327.

Campbell JL, Hornbeck JW, McDowell WH, Buso DC, Shanley J B, Likens GE 2000: Dissolved organic nitrogen budgets for upland forested ecosystems in New England, *Biogeochemistry* **49,** 123– 142.

Christopher SF, Mitchell MJ, McHale MR, Boyer EW, Burns DA, Kendall C 2008: Factors controlling nitrogen release from two forested catchments with contrasting hydrochemical responses. *Hydrol. Process.* **22,** 46–62

Cooper R, Thoss V, Watson H 2007: Factors influencing the release of dissolved organic carbon and dissolved forms of nitrogen from a small upland headwater during autumn runoff events. *Hydrol. Process.* **21,** 622–633

Creed IF, Band LE, Foster NW *et al.* 1996: Regulation of nitrite-N release from temperate forest: a test of N flushing hypothesis. *Water Resour. Res.* **32,** 3337-3354.

Creed IF, Band LE 1998a: Export of nitrogen from catchments within a temperate forest: evidence for a unifying mechanism regulated by variable source area dynamics. *Water Resour. Res.* **11,** 3105–3120.

Creed IF, Band LE 1998b: exporting functional similarity in the export of nitrite-N from forested catchments: a mechanistic modeling approach. *Water Recour. Res.* **34,** 3079-3093.

Geiger W 1987: Flushing effects in combined sewer systems. In: Proceedings of the 4th International Conference Urban Drainage, Lausanne, Switzerland, pp. 40–46.

Hagedorn F, Bucher J, Schleppi P 2001: Contrasting dynamics of dissolved inorganic

and organic nitrogen in soil and surface waters of forested catchments with Gleysols. *Geoderma* **100,** 173– 192.

Hagedorn F, Schleppi P, Waldner P, Fluhler H 2000: Export of dissolved organic carbon and nitrogen from Gleysol dominated catchments—The significance of water flow paths. *Biogeochemistry* **50,** 137–161.

Hatano R, Nagumo T, Hata H *et al*. 2005: Impact of nitrogen cycling on stream water quality in a basin associated with forest, grassland and animal husbandry, Hokkaido, Japan. *Ecol. Eng*. **24,** 509–515.

Hayakawa A, Shimizu MK, Woli KP, Kuramochi K, Hatano R 2006: Evaluating Stream Water Quality through Land Use Analysis in Two Grassland Catchments: Impact of Wetlands on Stream Nitrogen Concentration. *J. Environ. Qual.* **35,** 617–627.

Hayakawa A, Woli KP, Shimizu M, Nomaru K, Kuramochi K, Hatano R 2009: The nitrogen budget and relationships with riverine nitrogen exports of a dairy cattle farming catchment in eastern Hokkaido, Japan. *Soil Sci. Plant Nutr.*, In press.

Hill AR, Kemp WA, Buttle JM, Goodyear D 1999: Nitrogen chemistry of subsurface storm runoff on forested Canadian Shield hillslopes. *Water Resour. Res.* **35,** 811-821

Inamdar SP, Mitchell MJ 2006: Hydrologic and topographic controls on storm-event exports of dissolved organic carbon (DOC) and nitrate across catchment scales. *Water Resour. Res.* **42,** W03421, doi: 10.1029/2005WR004212.

Inamdar SP, Mitchell MJ 2007: Storm event exports of dissolved organic nitrogen

(DON) across multiple catchments in a glaciated forested watershed. *J. Geophys. Res.* **112,** G02014,doi:10.1029/2006JG000309.

Inamdar SP, Christopher SF, Mitchell MJ 2004: Export mechanisms for dissolved organic carbon and nitrate during storm events in a glaciated forested catchment in New York, USA. *Hydrol. Process.* **18,** 2651–2661.

Iqbal MZ 2002: Nitrate flux from aquifer storage in excess of baseflow contribution during a rain event. *Water Res.* **36,** 788–792.

Jia HY, Lei AL, Lei JS, *et al*. 2007: Effects of hydrological processes on nitrogen loss in purple soil. *Agr. Water Manage.* **89,** 89–97.

Jiang R, Zhu B, Tang JL, Luo ZX, Wang D, Xin W, Wei SQ 2008: Characteristics of nitrogen and phosphorus losses in typical rainfall-runoff events in a small watershed in hilly area of purple soil. *Journal of Agro-Environment Science* **27(4),** 1353-1358 (in Chinese with English summary).

Jiang R, Zhu B, Tang JL, Luo ZX 2009: Transportation processes and loss fluxes of nitrogen and phosphorous through storm runoff in a typical small watershed in the hilly area of purple soil. *Journal of hydraulic engineering* **40(6),** 659-666 (in Chinese with English summary).

Kondolf GM, Wilcock PR 1996: The flushing flow problem: defining and evaluating objectives. *Water Resour. Res.* **32,** 2589–2600.

Lee JH, Bang KW, Ketchum LH, Choe JS, Yu MJ 2002: First flush analysis of urban storm runoff. *Sci. Total Environ.* **293 (1-3),** 163-175.

Luo ZX 2008: Stormwater runoff pollution and its control mechanism of natural ditch in a rural township—a case study of Linshan rural township in the hilly area of purple soils, China. PhD dissertation of Chinese Academy of Sciences (in Chinese with English abstract).

McDonnell J, Owens IF, Stewart MK 1991: A case study of shallow flow paths in a steep zero-order basin. *Water Resour. Bull.* **27,** 679–685.

McHale MR, Mitchell MJ, McDonnell JJ, Cirmo CP 2000: Nitrogen solutes in an Adirondack watershed: Importance of dissolved organic nitrogen, *Biogeochemistry* **48(2),** 165– 184, doi:10.1023/A:1006121828108.

McHale M, McDonnell JJ, Mitchell MJ, Cirmo CP 2002: A field based study of soil- and groundwater nitrate release in an Adirondack forested watershed. *Water Resour. Res.* **38(4)**, 1029/2000 WR000102.

McNamara JP, Kane DL, Hobbie JE *et al*. 2008: Hydrologic and biogeochemical controls on the spatial and temporal patterns of nitrogen and phosphorus in the Kuparuk River, arctic Alaska. *Hydrol. Process.* **22,** 3294–3309.

Mitchell MJ, Raynal DJ, Driscoll CT 1996: Biogeochemistry of a forested watershed in the central Adirondack Mountains: temporal changes and mass balances. *Water, Air, and Soil Pollut.* **88,** 355–369.

Ocampo CJ, Oldham CE, Sivapalan M, *et al*. 2006: hydrological versus biogeochemical controls on catchment nitrate export: a test of the flushing mechanism. *Hydrol. Process.* **20,** 4269-4286

Ohte N, Tokuchi N, Katsuyama M, Hobara S, Asano Y, Koba K 2003: Episodic increase in nitrate concentrations in streamwater due to the partial dieback of a pine forest in Japan: runoff generation processes control seasonality. *Hydrol. process.* **17,** 237-249.

Qualls RG, Haines BL 1991: Geochemistry of dissolved organic nutrients in water percolating through a forest ecosystem. *Soil Sci. Soc. Am. J.* **55**, 1112–1123.

Rusjan S, Brilly M, Mikos M 2008: Flushing of nitrate from a forested watershed: An insight into hydrological nitrate mobilization mechanisms through seasonal high-frequency stream nitrate dynamics. *J, Hydrol.* **354,** 187– 202

Saget A, Chebbo G, Bertrand-Krajewski J 1995: The first flush in sewer system. In: Proceedings of the 4th International Conference Sewer Solids-Characteristics, Movement, Effects and Control, Dundee, UK, pp. 58–65.

Sebestyen, SD, Boyer EW, Shanley JB, Kendall C, Doctor DH, Aiken GR, Ohte N 2008: Sources, transformations, and hydrological processes that control stream nitrate and dissolved organic matter concentrations during snowmelt in an upland forest, *Water Resour. Res.* **44,** W12410, doi: 10.1029/2008WR006983.

Vanderbilt KL, Lajtha K, Swanson FJ 2003: Biogeochemistry of unpolluted forested watersheds in the Oregon Cascades: Temporal patterns of precipitation and stream nitrogen fluxes, *Biogeochemistry* **62**, 87– 117.

Weiler M, McDonnell JJ 2006: Testing nutrient flushing hypotheses at the hillslope scale: a virtual experiment approach. *J. Hydrol.* **319**, 339–356.

Willett VB, Reynolds BA, Stevens PA, Ormerod SJ, Jones DL 2004: Dissolved organic nitrogen regulation in freshwaters, *J. Environ. Qual.* **33,** 201– 209.

Woli, KP, NagumoT, Kuramochi K, Hatano R 2004: Evaluating river water quality through land use analysis and N budget approaches in livestock farming areas. *Sci. Total Environ.* **329,** 61–74.

Zhang Z, Fukushima T, Onda Y *et al*. 2007: Nutrient runoff from forested watersheds in central Japan during typhoon storms: implications for understanding runoff mechanisms during storm events. *Hydrol. Process.* **21,** 1167–1178

Zhang Z, Fukushima T, Onda Y, *et al*. 2008: Characterisation of diffuse pollutions from forested watersheds in Japan during storm events — its association with rainfall and watershed features. *Sci. Total Environ.* **390,** 215-226.

**Figure legends**

**Figure 1** Location of the study watershed and water sampling site.

**Figure 2** Precipitation, stream discharge, and ground water level (only one well is shown, the others are similar) during storm events in 2003.

**Figure 3** The ratio of PN: $NO_3^-$-N during storm events.

**Figure 4** Temporal changes in N and SS concentrations, discharge, rainfall, and shallow groundwater level during storm events.

**Figure 5** Patterns of N and SS during storm events. Arrows indicate the time course.

**Figure 6** M (V) curve: normalized mass first flush relative to normalized discharge.

**Figure 7** Concentrations of Si and $NO_3$-N during storm events.

**Figure 8** $NO_3^-$-N concentrations in soil profile (ANOVA, $p<0.05$, $n=27$).

**Figure 9** Concentrations of $NO_3^-$-N and DON, and shallow ground water level during storm events.

686 **Table 1** Characteristics of each hydrological storm event in the study area

| Storm event | Date | Precipitation | | Rainfall duration | [a]$API_x$ | | Discharge | | | % of annual discharge | Runoff coefficient |
|---|---|---|---|---|---|---|---|---|---|---|---|
| | | Total (mm) | Max (mm $h^{-1}$) | (h) | $API_7$ | $API_{21}$ | Total ($\times 10^6$ $m^3$) | Peak ($m^3$ $s^{-1}$) | [b]$T_p$ (h) | | |
| E1 | 2003/6/20-2003/6/23 | 80 | 11 | 16 | 3.2 | 5.2 | 10.6 | 51.4 | 14 | 1.31 | 0.195 |
| E2 | 2003/7/11-2003/7/14 | 91 | 11 | 23 | 0.0 | 6.6 | 53.8 | 167.7 | 16 | 6.65 | 0.870 |
| E3 | 2003/9/30-2003/10/3 | 55 | 15 | 15 | 19.3 | 28.4 | 39.1 | 122.6 | 9 | 4.83 | 1.047 |
| E4 | 2003/10/23-2003/10/25 | 50 | 8 | 19 | 1.9 | 2.6 | 38.6 | 135.8 | 11 | 4.77 | 1.136 |

[a] $API_x$: Antecedent precipitation index determined for 7 and 14 preceding days.

[b] $T_p$: Time to peak (the time from the outset of rain to the peak of stream water discharge)

E1, E2, E3, and E4 represent the storm events on June 20, July 11, September 30, and October 23 in 2003, respectively.

687

**Table 2** Discharge, SS, and N concentrations during the storm and base flow events. Different superscript letters (a, b, and c) followed by median values indicate significant difference (Steel-Dwass test, $p<0.05$)

| Storm events | | Discharge ($m^3\ s^{-1}$) | SS (mg $L^{-1}$) | $NO_3^-$-N (mg $L^{-1}$) | TN (mg $L^{-1}$) | DON (mg $L^{-1}$) | PN (mg $L^{-1}$) | $NH_4^+$-N (mg $L^{-1}$) | $NO_3^-$-N /TN(%) | DON /TN(%) | PN /TN(%) |
|---|---|---|---|---|---|---|---|---|---|---|---|
| E1 | Mean | 32.0 | 34.1 | 0.6 | 1.7 | 0.3 | 0.8 | 0.006 | 37 | 16 | 46 |
| | Median | $28.1^{a}$ | $15.7^{ac}$ | $0.5^{a}$ | $1.5^{a}$ | $0.2^{a}$ | $0.6^{a}$ | $0.002^{ac}$ | | | |
| | Min | 22.6 | 6.8 | 0.5 | 1.0 | 0.1 | 0.3 | 0.0 | | | |
| | Max | 51.4 | 141.7 | 0.8 | 3.8 | 0.6 | 2.7 | 0.02 | | | |
| E2 | Mean | 64.8 | 327.9 | 0.5 | 2.7 | 0. 3 | 1.9 | 0.009 | 27 | 15 | 57 |
| | Median | $50.2^{b}$ | $81.5^{b}$ | $0.4^{b}$ | $1.6^{a}$ | $0.3^{b}$ | $0.9^{a}$ | $0.007^{a}$ | | | |
| | Min | 22.0 | 13.1 | 0.3 | 0.9 | 0.1 | 0.2 | 0.0 | | | |
| | Max | 167.7 | 1596.1 | 0.7 | 8.7 | 0.5 | 7.5 | 0.02 | | | |
| E3 | Mean | 54.3 | 100 | 0.6 | 1.5 | 0. 4 | 0.6 | 0.002 | 50 | 30 | 20 |
| | Median | $41.6^{b}$ | $31.3^{ab}$ | $0.5^{a}$ | $1.0^{a}$ | $0.3^{a}$ | $0.1^{b}$ | $0.0^{bc}$ | | | |
| | Min | 31.6 | 13.3 | 0.5 | 0.7 | 0.2 | 0.0 | 0.0 | | | |
| | Max | 122.6 | 509.5 | 1.0 | 4.5 | 0.8 | 3.2 | 0.04 | | | |
| E4 | Mean | 50.8 | 152 | 0.6 | 1.6 | 0.4 | 0.6 | 0.004 | 45 | 34 | 21 |
| | Median | $43.9^{ab}$ | $25.0^{abc}$ | $0.5^{ab}$ | $1.0^{a}$ | $0.4^{b}$ | $0.2^{b}$ | $0.0^{c}$ | | | |
| | Min | 23.3 | 1.5 | 0.4 | 0.7 | 0.3 | 0.0 | 0.0 | | | |
| | Max | 135.8 | 856.2 | 0.8 | 4.2 | 0.7 | 2.7 | 0.02 | | | |
| Baseflow | Mean | 22.9 | 9.3 | 0.6 | 1.1 | 0.4 | 0.1 | 0.002 | 54 | 36 | 9 |
| | Median | $20.2^{a}$ | $7.0^{c}$ | $0.6^{ab}$ | $1.0^{a}$ | $0.4^{ab}$ | $0.1^{b}$ | $0.0^{c}$ | | | |
| | Min | 19.4 | 5.8 | 0.4 | 0.9 | 0.2 | 0.0 | 0.0 | | | |
| | Max | 32.0 | 17.5 | 0.7 | 1.4 | 0.6 | 0.2 | 0.03 | | | |

Deleted: events

Deleted: Median values followed by

Deleted: d

692 **Table 3** Pearson correlation coefficients (r) between discharge-weighted mean
693 concentrations of SS and N and rainfall condition during the rising limb of discharge in
694 each storm events

| Storm event | r value for the N concentration and rainfall intensity | | | | r value for the N concentration and accumulative rainfall | | | |
|---|---|---|---|---|---|---|---|---|
| | SS | $NO_3^-$-N | DON | PN | SS | $NO_3^-$-N | DON | PN |
| E1 | -0.768** | -0.724* | -0.807** | -0.622 | 0.893** | 0.882** | 0.768** | 0.768** |
| E2 | -0.794** | -0.282 | -0.702* | -0.713* | 0.881** | 0.865** | 0.928** | 0.912** |
| E3 | -0.323 | -0.307 | -0.583 | -0.426 | 0.741* | 0.784* | 0.912** | 0.812* |
| E4 | -0.177 | -0.038 | -0.146 | -0.162 | 0.871** | 0.898** | 0.879** | 0.878** |

**P<0.01; *p<0.05

695

696 **Table 4** Summary statistics for regressions describing the exponential decline (k) in the
697 concentrations of N during storm events

| | Storm event | k ($h^{-1}$) | $r^2$ | Time constant $t_{1/e}$ (h) |
|---|---|---|---|---|
| SS | E1 | -0.039±0.007 | 0.72±0.48 | 25.87±3.93 |
| | E2 | -0.071±0.007 | 0.89±0.48 | 14.01±1.26 |
| | E3 | -0.203±0.022 | 0.84±0.49 | 4.92±0.49 |
| | E4 | -0.463±0.122 | 0.67±0.94 | 2.16±0.45 |
| | Average | -0.194±0.039 | 0.78±0.59 | 11.74±1.53 |
| $NO_3^-$-N | E1 | -0.010±0.001 | 0.90±0.06 | 97.35±9.00 |
| | E2 | -0.038±0.005 | 0.81±0.09 | 26.10±3.13 |
| | E3 | -0.036±0.010 | 0.53±0.14 | 27.48±6.11 |
| | E4 | -0.063±0.016 | 0.66±0.15 | 15.86±3.20 |
| | Average | -0.037±0.008 | 0.72±0.11 | 41.70±5.36 |
| DON | E1 | -0.019±0.002 | 0.84±0.15 | 52.64±6.08 |
| | E2 | -0.083±0.012 | 0.78±0.20 | 12.00±1.52 |
| | E3 | -0.081±0.012 | 0.82±0.16 | 12.39±1.55 |
| | E4 | -0.156±0.019 | 0.93±0.10 | 6.43±0.72 |
| | Average | -0.085±0.011 | 0.84±0.15 | 20.87±2.47 |
| PN | E1 | -0.035±0.005 | 0.79±0.33 | 28.29±3.67 |
| | E2 | -0.245±0.018 | 0.94±0.29 | 4.09±0.27 |
| | E3 | - | - | - |
| | E4 | - | - | - |
| | Average | -0.139±0.011 | 0.86±0.31 | 16.19±1.97 |

698

699 **Table 5** $MFF_{30}$ and $MFF_{50}$ for quantifying the magnitude of first flush

| Storm event | $MFF_{30}$ | | | | | $MFF_{50}$ | | | | |
|---|---|---|---|---|---|---|---|---|---|---|
| | $NO_3^-$-N | DON | TN | PN | SS | $NO_3^-$-N | DON | TN | PN | SS |
| E1 | 1.13 | 1.23 | 1.50 | 1.87 | 2.17 | 1.14 | 1.22 | 1.34 | 1.54 | 1.64 |
| E2 | 1.20 | 1.37 | 1.90 | 2.17 | 2.30 | 1.14 | 1.30 | 1.60 | 1.74 | 1.82 |
| E3 | 1.20 | 1.37 | 1.77 | 2.87 | 2.50 | 1.12 | 1.28 | 1.40 | 1.72 | 1.88 |
| E4 | 1.17 | 1.27 | 1.37 | 1.87 | 2.43 | 1.10 | 1.26 | 1.24 | 1.42 | 1.66 |

700

701 **Table 6** N loads during storm events and percentage of annual load

| | Load (kg) | | | | | % of annual load | | | | |
|---|---|---|---|---|---|---|---|---|---|---|
| | SS | TN | $NO_3$-N | DON | PN | SS | TN | $NO_3$-N | DON | PN |
| E1 | 396.4 | 18.3 | 6.3 | 3.3 | 8.6 | 0.5 | 1.7 | 1.3 | 1.4 | 2.3 |
| E2 | 25196.8 | 168.4 | 24.9 | 17.9 | 125.0 | 29.3 | 15.5 | 5.3 | 7.7 | 34.0 |
| E3 | 3014.8 | 56.9 | 23.6 | 15.6 | 17.9 | 3.5 | 5.2 | 5.0 | 6.7 | 4.9 |
| E4 | 3342.9 | 58.0 | 21.7 | 20.7 | 15.6 | 3.9 | 5.3 | 4.6 | 8.9 | 4.2 |
| Total | 31950.9 | 301.6 | 76.5 | 57.5 | 167.1 | 37.2 | 27.7 | 16.2 | 24.7 | 45.4 |

702

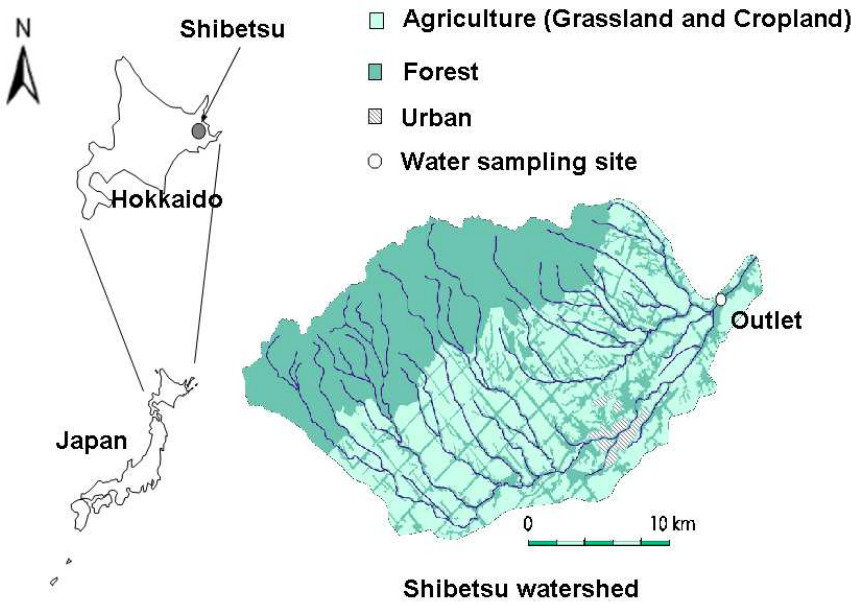


figure 1 Location of the study watershed and water sampling site
254x190mm (96 x 96 DPI)

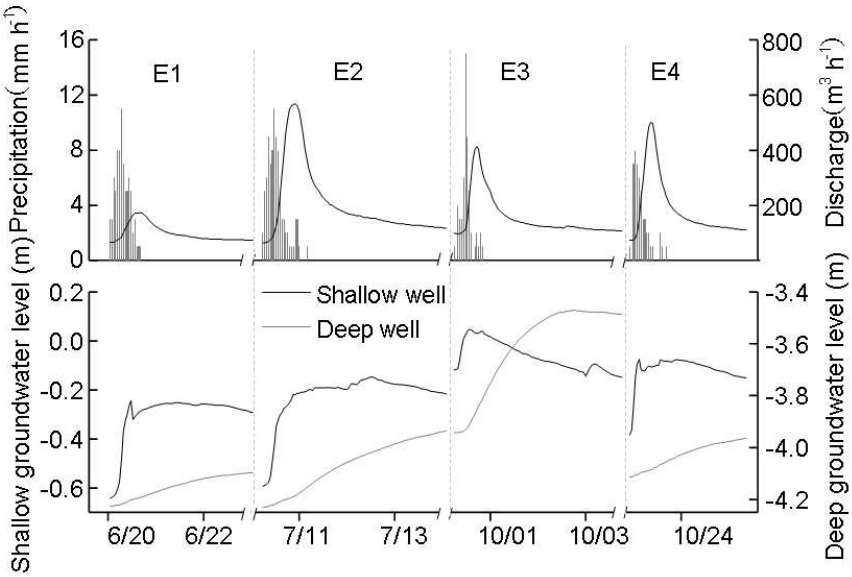


figure 2 Precipitation, stream discharge, and ground water level (only one well is shown, the others are similar) during storm events in 2003
254x190mm (96 x 96 DPI)

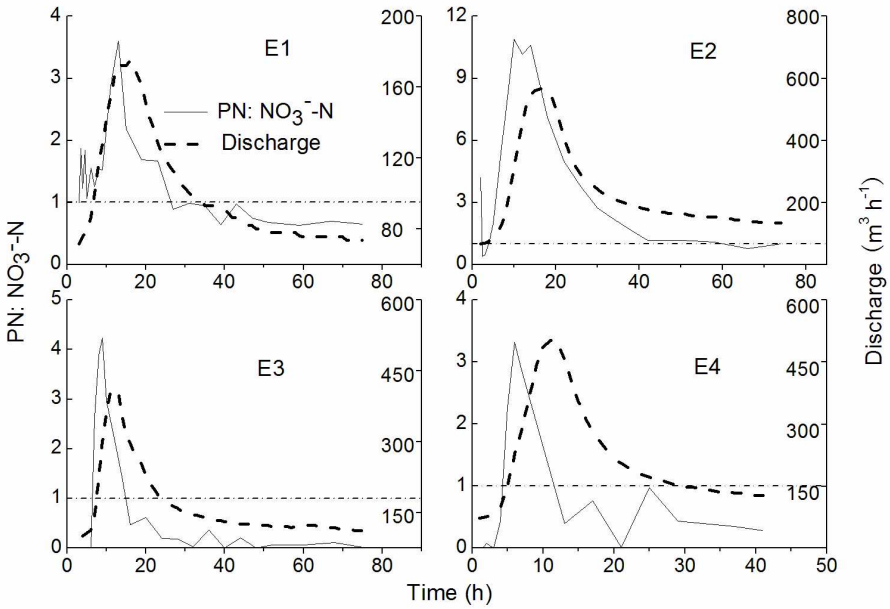


figure 3 The ratio of PN: $NO_3^-$-N during storm events
284x201mm (150 x 150 DPI)

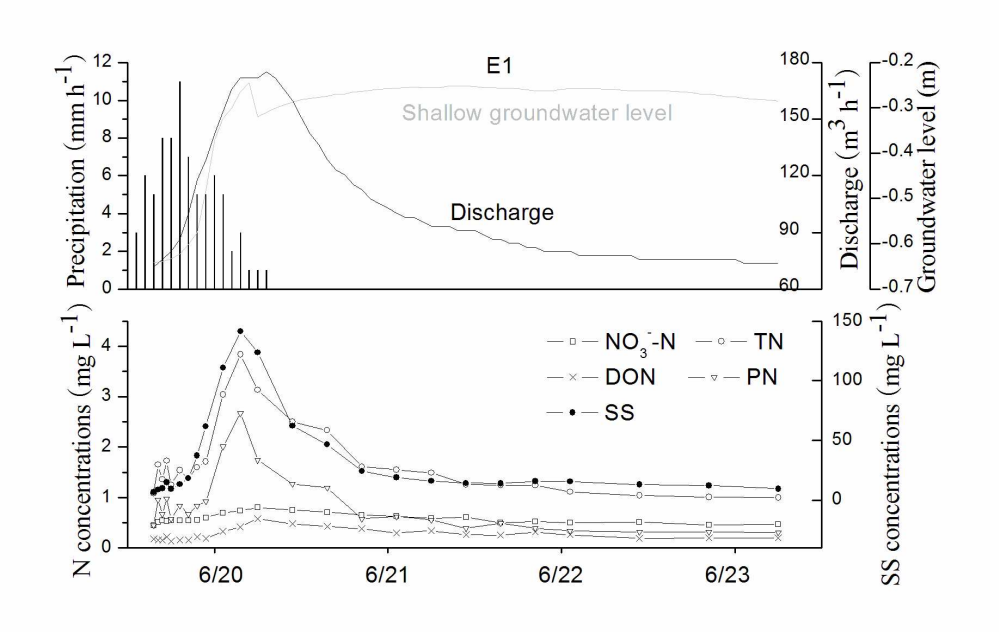


311x198mm (150 x 150 DPI)

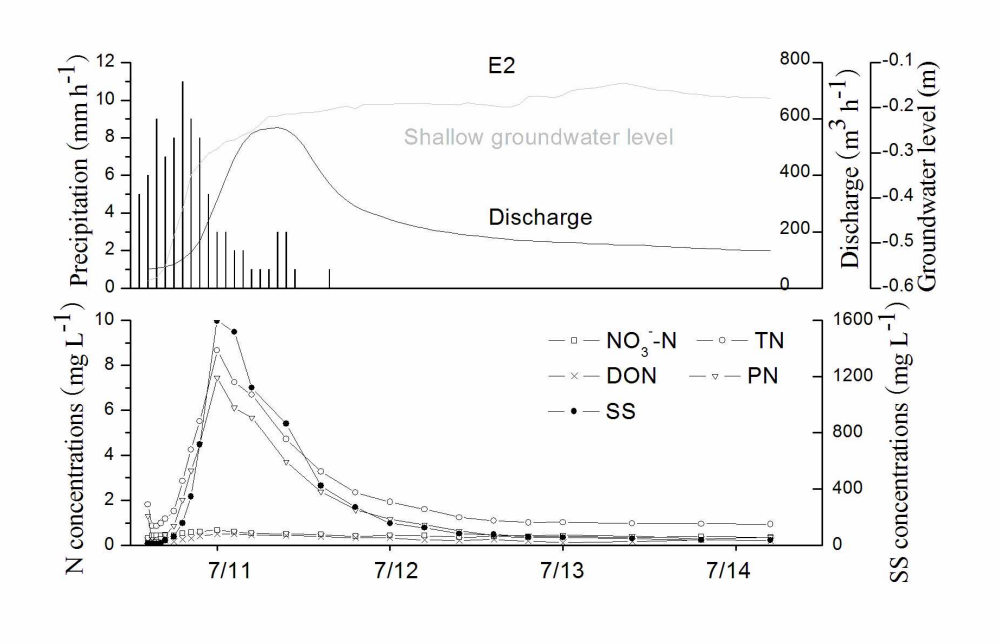


312x202mm (150 x 150 DPI)

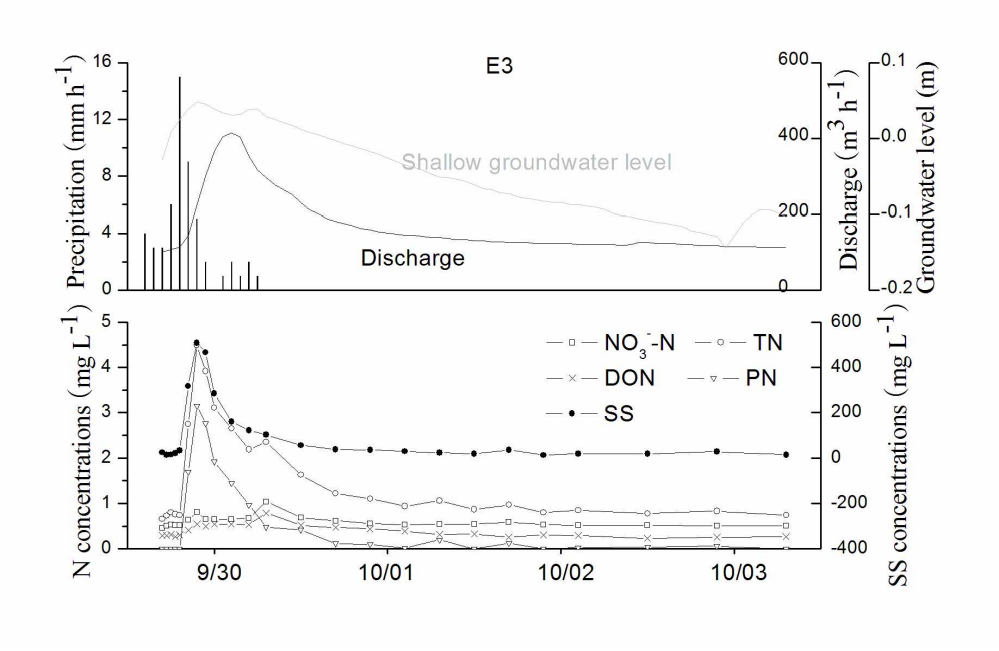


311x202mm (150 x 150 DPI)

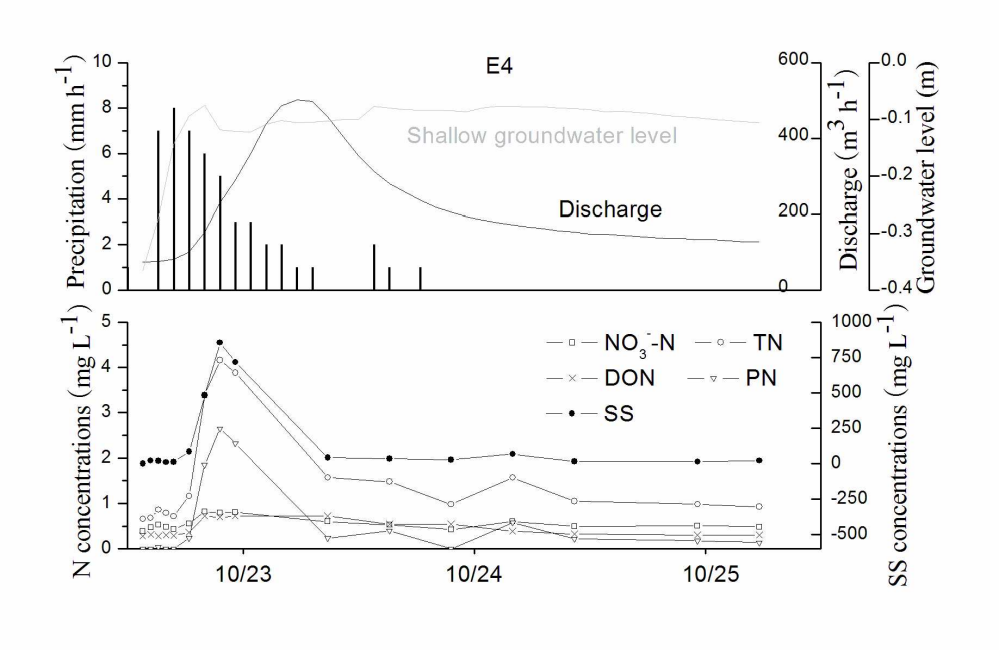


figure 4 Temporal changes in N and SS concentrations, discharge, rainfall, and shallow groundwater level during storm events
311x202mm (150 x 150 DPI)

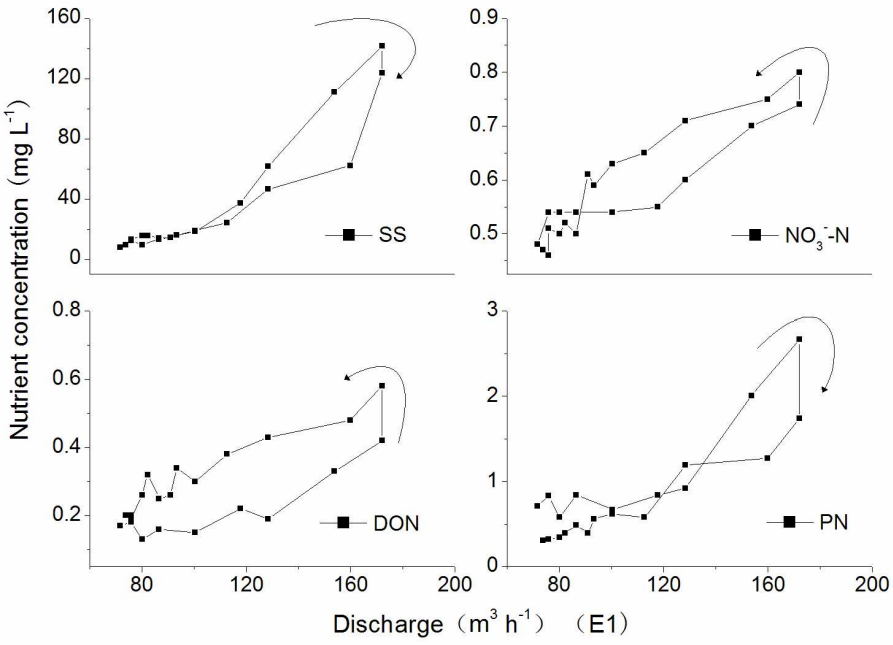


275x204mm (150 x 150 DPI)

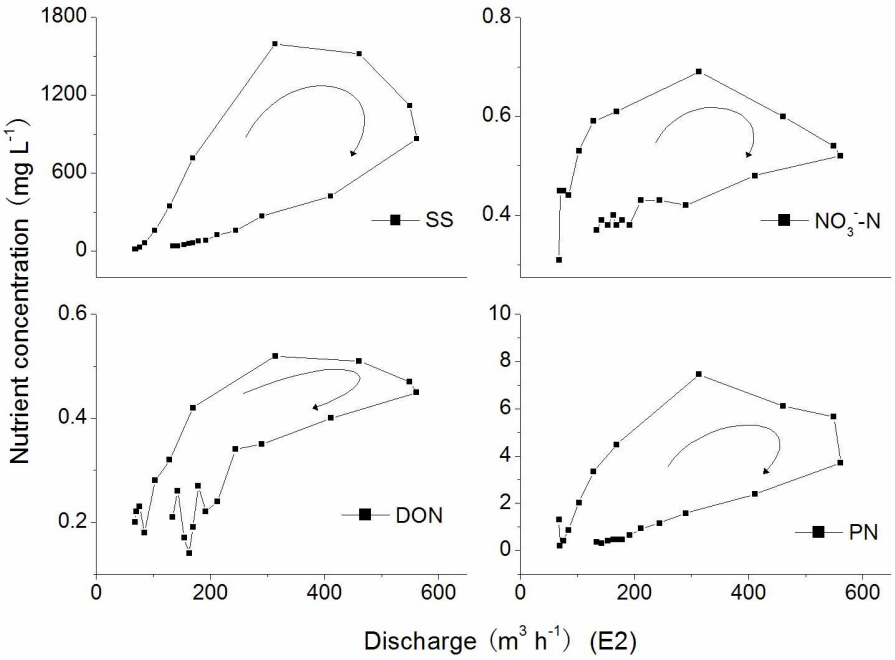


271x207mm (150 x 150 DPI)

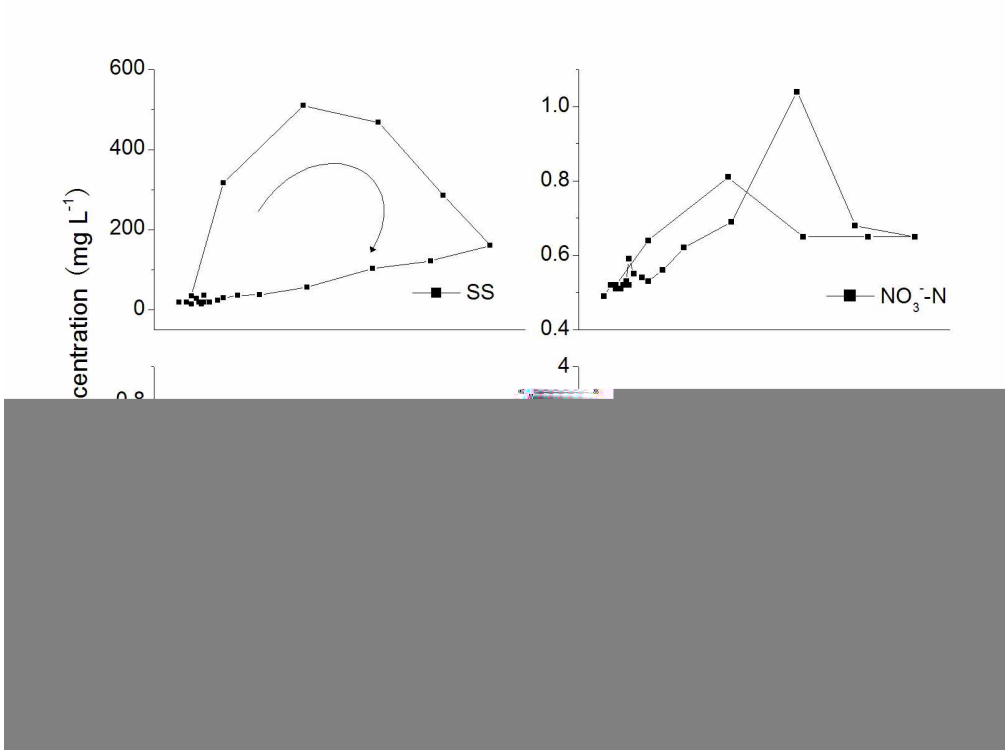


271x203mm (150 x 150 DPI)

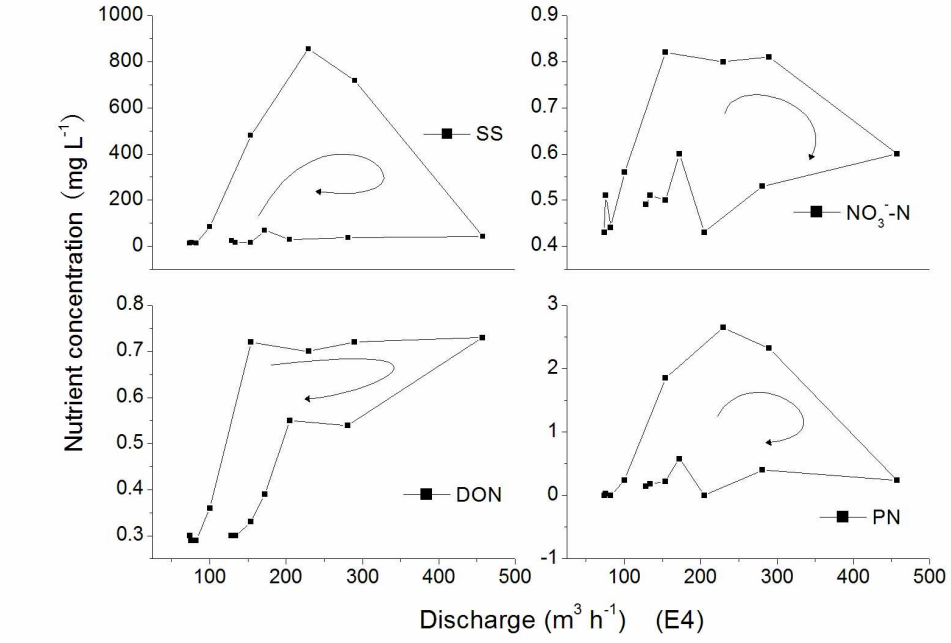


figure 5 Patterns of N and SS during storm events. Arrows indicate the time course
278x206mm (150 x 150 DPI)

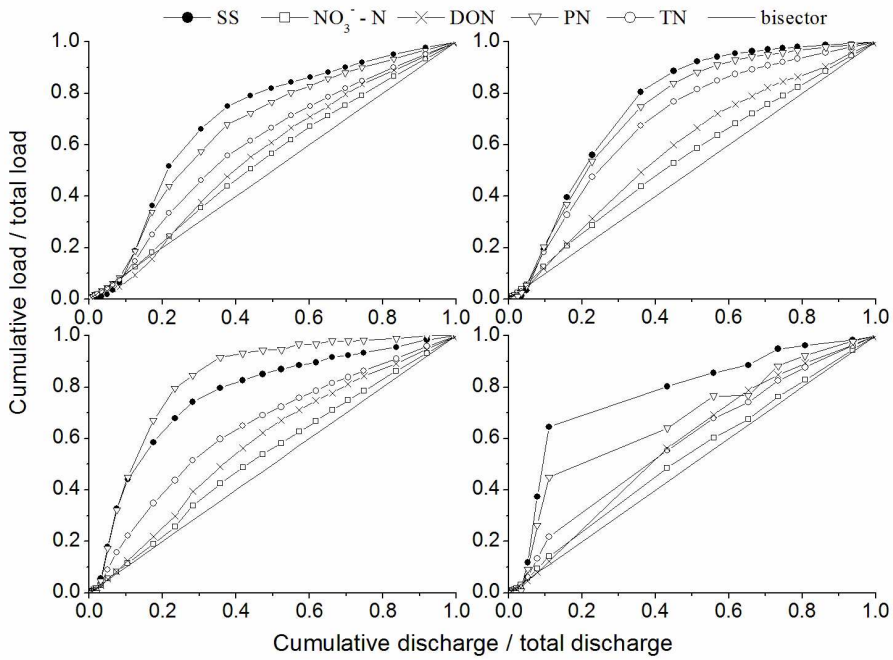


figure 6 M (V) curve: normalized mass first flush relative to normalized discharge
274x209mm (150 x 150 DPI)

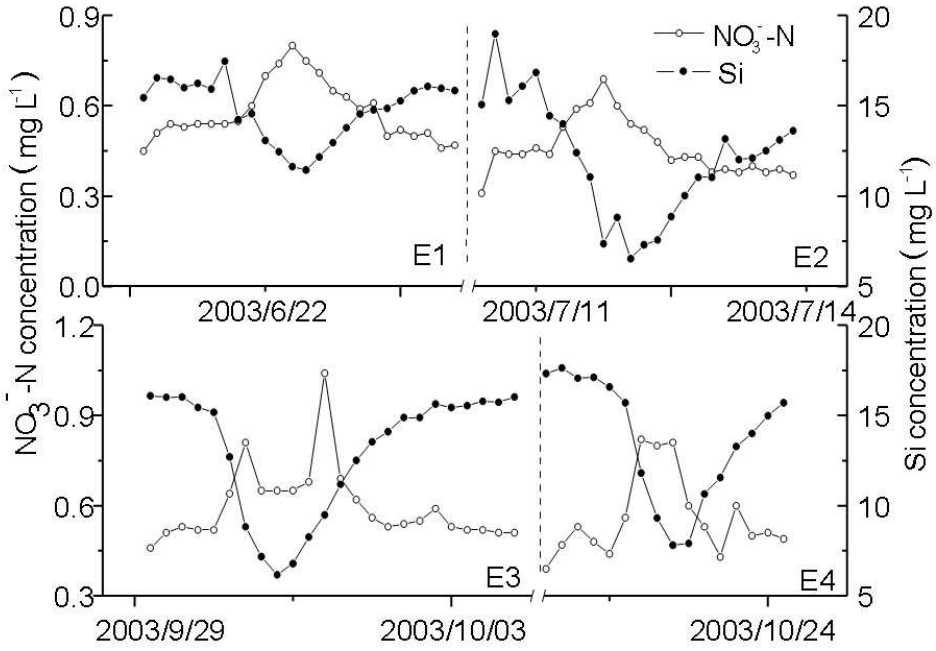


figure 7 Concentrations of Si and $NO_3^-$-N during storm events
254x190mm (96 x 96 DPI)

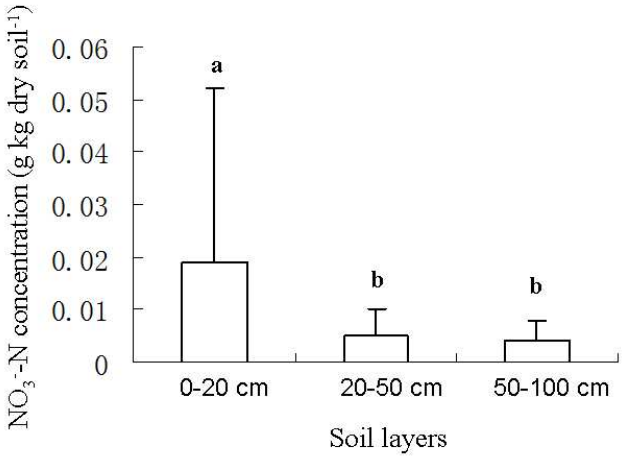


figure 8 $NO_3^-$-N concentrations in soil profile (ANOVA, $p<0.05$, n=27)
254x190mm (96 x 96 DPI)

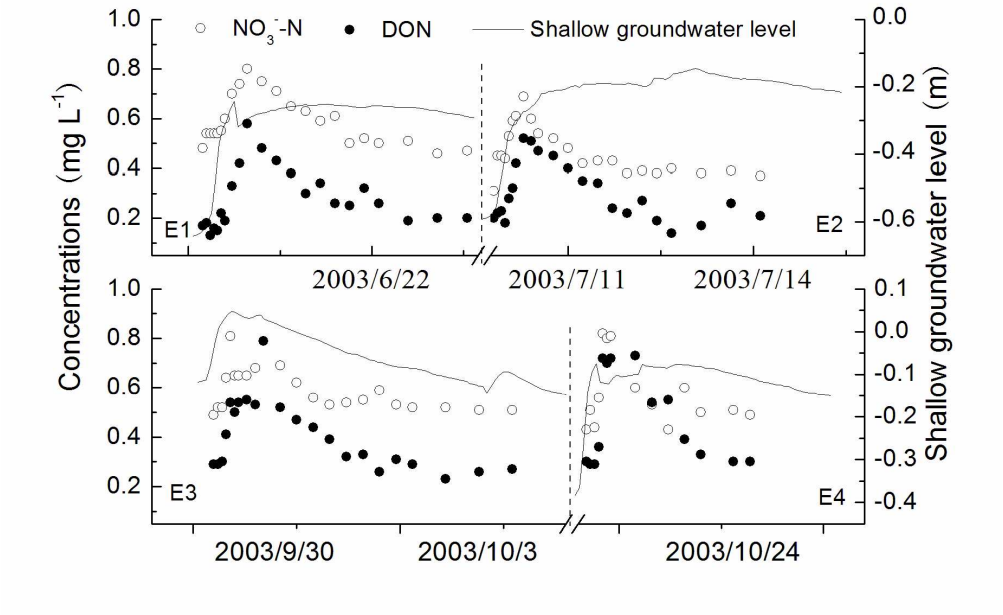


figure 9 Concentrations of $NO_3^-$-N and DON, and shallow ground water level during storm events
312x207mm (150 x 150 DPI)